BJ www.biochemj.org

BJ Metabolism

Biochem. J. (2011) **435**, 267–276 (Printed in Great Britain) doi:10.1042/BJ20101867

online data

267

A lipidomic screen of palmitate-treated MIN6 β-cells links sphingolipid metabolites with endoplasmic reticulum (ER) stress and impaired protein trafficking

Ebru BOSLEM*†, Gemma MacINTOSH‡, Amanda M. PRESTON*†, Clarissa BARTLEY*, Anna K. BUSCH*, Maria FULLER§, D. Ross LAYBUTT*†, Peter J. MEIKLE‡ and Trevor J. BIDEN*†[1]

*Diabetes and Obesity Program, Garvan Institute of Medical Research, 384 Victoria Street, Darlinghurst, NSW 2010, Australia, †St Vincent's Clinical School, Faculty of Medicine, University of New South Wales, Sydney, NSW, Australia, ‡Baker IDI Heart and Diabetes Institute, Commercial Road, Melbourne, Australia, and §Department of Genetic Medicine, Children, Youth and Women's Health Service, 72 King William Road, Adelaide, SA 5006, Australia

Saturated fatty acids promote lipotoxic ER (endoplasmic reticulum) stress in pancreatic β-cells in association with Type 2 diabetes. To address the underlying mechanisms we employed MS in a comprehensive lipidomic screen of MIN6 β-cells treated for 48 h with palmitate. Both the overall mass and the degree of saturation of major neutral lipids and phospholipids were only modestly increased by palmitate. The mass of GlcCer (glucosylceramide) was augmented by 70% under these conditions, without any significant alteration in the amounts of either ceramide or sphingomyelin. However, flux into ceramide (measured by [^{3}H]serine incorporation) was augmented by chronic palmitate, and inhibition of ceramide synthesis decreased both ER stress and apoptosis. ER-to-Golgi protein trafficking was also reduced by palmitate pre-treatment, but was overcome by overexpression of GlcCer synthase. This was accompanied by increased conversion of ceramide into GlcCer, and reduced ER stress and apoptosis, but no change in phospholipid desaturation. Sphingolipid alterations due to palmitate were not secondary to ER stress since they were neither reproduced by pharmacological ER stressors nor overcome using the chemical chaperone phenylbutyric acid. In conclusion, alterations in sphingolipid, rather than phospholipid, metabolism are more likely to be implicated in the defective protein trafficking and enhanced ER stress and apoptosis of lipotoxic β-cells.

Key words: apoptosis, ceramide, endoplasmic reticulum stress, islet, lipidomics, lipotoxicity, palmitate, pancreatic β-cell, trafficking, Type 2 diabetes.

INTRODUCTION

Type 2 diabetes is associated with obesity and is characterized by insulin resistance of peripheral tissues such as muscle, liver and adipose tissue. Generally the pancreatic β-cell compensates for this insulin resistance by increasing insulin output, except in a minority of susceptible individuals, where β-cell mass and function decline such that insufficient insulin is provided to control blood glucose [1–3]. It is generally accepted that prolonged exposure to circulatory FAs (fatty acids) and the accumulation of lipids at sites other than adipose tissue, contributes to both insulin resistance and β-cell dysfunction [1,4]. The latter comprises both insulin secretory defects and a relative loss of β-cell mass due to apoptosis [5]. Whereas both saturated and unsaturated FAs contribute to the secretory dysfunction, specifically saturated species, such as palmitate, mediate lipotoxic apoptosis [6–10], and in fact unsaturated species are protective [5–7,11–13].

Previous studies have strongly linked ER (endoplasmic reticulum) stress with β-cell apoptosis [14,15]. The UPR (unfolded protein response), triggered by the accumulation of misfolded proteins in the ER, is the signalling network responsible for transducing ER stress, and leads initially to improved folding and degradation of misfolded proteins. If this adaptive response is insufficient, and chronic ER stress persists, apoptosis is initiated [14,15]. The pathophysiological relevance of ER stress is highlighted by its presence in β-cells of *db*/*db* mice, a model of Type 2 diabetes [9]. Moreover, increased ER stress markers were also observed in islets of human subjects with diabetes [9]. Although enhanced secretory demand to compensate for insulin resistance would certainly contribute under these conditions, there is also an intrinsic effect of FAs on the β-cell, in particular saturated FAs, to promote ER stress [8–10]. This in turn mediates apoptosis by induction of the transcription factor CHOP [C/EBP (CCAAT/enhancer-binding protein)-homologous protein 10] [10,16,17]. Moreover, studies using genetic intervention or chemical chaperones have shown that ER stress is a major contributor to apoptosis in mild models of β-cell lipotoxicity [9,10,16]. The mechanisms whereby saturated FAs induce ER stress are unclear, although impairment of protein folding due to inhibition of SERCA (sarcoplasmic/endoplasmic reticulum Ca^{2+}-ATPase) pump activity and resultant depletion of ER calcium has been proposed [10]. On the other hand the capacity of different FAs to promote calcium depletion is not strictly proportional to the accompanying ER stress [8,10], and ER protein misfolding is not readily observed in mild models of β-cell lipotoxicity [18]. We have therefore proposed

Abbreviations used: BCA, bicinchoninic acid; CE, cholesteryl ester; Cer, ceramide; CHOP, C/EBP (CCAAT/enhancer-binding protein)-homologous protein 10; CM-H_2DCFDA, 5-(and 6)-chloromethyl-2′,7′-dichlorodihydrofluorescein diacetate; DAG, diacylglycerol; DMEM, Dulbecco's modified Eagle's medium; ER, endoplasmic reticulum; FA, fatty acid, GCS, glucosylceramide synthase; GFP, green fluorescent protein; GlcCer, glucosylceramide; GM130, *cis*-Golgi matrix protein of 130 kDa; HBSS, Hanks buffered salt solution; HPTLC, high-performance TLC; LacCer, lactosylceramide; NBD, 6-(*N*-7-nitrobenz-2-oxa-1,3-diazyl-4-yl)amino; NL, neutral loss; PBA, 4-phenylbutyric acid; PC, phosphatidylcholine; PE, phosphatidylethanolamine; PG, phosphatidylglycerol; PI, phosphatidylinositol; PR, palmitate-resistant; PS, phosphatidylserine; ROS, reactive oxygen species; SM, sphingomyelin; SPT1, serine palmitoyltransferase 1; TAG, triacylglycerol; THC, trihexosylceramide; VSVG, vesicular stomatis viral glycoprotein temperature-sensitive mutant.

[1] To whom correspondence should be addressed (email t.biden@garvan.org.au).

an additional mechanism involving protein overload, which is secondary to reductions in ER-to-Golgi protein trafficking [18].

Despite this progress, it remains uncertain how palmitate actually initiates ER stress and apoptosis in β-cells, beyond the knowledge that FA metabolism is required and that esterification pathways in particular are associated with creation of toxic metabolites [19]. Studies using yeast and tumour cells have led to the proposal that enhanced saturation of phospholipids, in particular PC (phosphatidylcholine), contributes to lipotoxic ER stress [20–22]. However, this has never been addressed in β-cells. Another possibility is the generation of Cer (ceramide) [23]. This sphingolipid has an established role as a pro-apoptotic lipid [24] and it can also enhance ER stress in some cell types, but not others [25,26]. Although little investigated in the context of ER stress, Cer has been implicated in β-cell apoptosis, mainly using the obese ZDF (Zucker diabetic fatty) rat model of Type 2 diabetes [27,28]. However, the pancreatic islets of these animals display profound perturbations in lipid handling, so this might represent an extreme case. Indeed, evidence for involvement of Cer in milder models of β-cell lipotoxicity is less strong [6,29–32], nor is a putative mechanism for the pro-apoptotic function of Cer readily apparent. Even less is known of the potential involvement of other sphingolipids such as SM (sphingomyelin) and GlcCer (glucosylceramide). The latter is generated by the enzyme GCS (GlcCer synthase) and is pro-apoptotic in some cell types [24,33]. Other glycosylated metabolites include LacCer (lactosylceramide) and THC (trihexosylceramide).

In the present study we sought to investigate the early metabolic events that underlie initiation of lipotoxic apoptosis in β-cells. Using MIN6 cells chronically exposed to palmitate we provide the first comprehensive analysis of accompanying alterations in the three major lipid classes: neutral lipids, phospholipids and sphingolipids. Our results strongly implicate alterations in sphingolipid metabolism in the induction of both terminal ER stress and apoptosis under these conditions, and further link these processes to defects in vesicular trafficking via the early secretory pathway.

EXPERIMENTAL

Reagents

All tissue culture media, supplements and trypsin for MIN6 cells were purchased from Gibco. Cell Death ELISA^{PLUS} kit, SYBR Green I and protease inhibitor tablets were obtained from Roche Diagnostics. Sources of other reagents were as follows: sodium palmitate, sodium orthovanadate, FA-free fraction V BSA, sucrose, sodium oleate, myriocin, PBA (4-phenylbutyric acid), cycloserine, cycloheximide and thapsigargin were from Sigma–Aldrich. Tunicamycin was from Biomol. Solution V, control pmaxGFP (GFP is green fluorescent protein) and the Nucleofector instrument were from Amaxa Biosystems. The GCS construct (in pCMWSport6, Clone ID #BC050828.1) was from American Tissue Culture Collection. NBD [6-(*N*-7-nitrobenz-2-oxa-1,3-diazyl-4-yl)amino]–Cer (#N2261), CM-H_2DCFDA [5-(and 6)-chloromethyl-2′,7′-dichlorodihydrofluorescein diacetate; #C-6827], pre-cast NuPAGE gels, sample buffer, reducing agent, antioxidant, electrophoresis tank and the transfer system for immunoblotting were from Invitrogen. The BCA (bicinchoninic acid) protein assay kit was from Pierce. Black 96-well assay plates were from Nunc.

Cell culture and chronic cell treatments

The mouse MIN6 insulinoma cell line and PR (palmitate-resistant) cell line were routinely passaged and cultured as described previously [11,34]. In brief, chronic palmitate treatment involved culture for 48 h in DMEM (Dulbecco's modified Eagle's medium; 6 mM glucose) with either 0.4 mM lipid pre-coupled to 0.92 g/100 ml BSA, for most MIN6 experiments, or 1 mM lipid pre-coupled to 2.3 g/100 ml BSA for PR cell experiments or their corresponding MIN6 controls passaged in parallel, as well as BSA-only controls. The lipid couplings were prepared at a 3:1 palmitate/BSA molar ratio [34]. The medium was replaced with fresh complete medium and lipid at 24 h. Cells for immunoblotting experiments were seeded in six-well plates at 8×10^5 cells per well in 3 ml. Apoptosis assays were performed in either a 96-well plate or 24-well plate format, at 3×10^4 cells per well (0.2 ml) or 2×10^5 cells per well (0.5 ml) respectively. MIN6 cells were seeded in 15 cm^2 tissue culture dishes at 1.6×10^7 cells per dish in 23 ml for lipid-profile studies. For overexpression studies, MIN6 cells were nucleofected with control pmaxGFP construct or GCS construct in solution V, using program G16 (Amaxa Biosystems) [9] prior to plating in test dishes as indicated above. Other chronic (24 h) treatments in DMEM included thapsigargin at a final concentration of 50 nM, tunicamycin at 2 μM, PBA at 5 mM, cycloserine at 0.5 mM and myriocin at 100 nM.

Apoptosis assay

MIN6 cells treated with chronic palmitate were harvested as described previously [16] in lysis buffer provided in the Cell Death ELISA^{PLUS} kit. Histone-bound mono- and oligo-nucleosomes were quantified according to the kit manufacturer's instructions. The absorbance for each apoptosis sample was adjusted for total DNA content, as measured by SYBR Green I intercalation of the remaining sample, and quantified against a salmon sperm DNA standard curve following excitation/emission (at 485 nm/520 nm).

Metabolic flux assays: NBD–Cer and [^{3}H]serine

An assay of GCS was performed with a method adapted from that described by Boath et al. [35]. Briefly, MIN6 cells in 24-well plates were labelled with 3 μM NBD–Cer (Invitrogen) for 1 h or 40 μCi of [G-^{3}H]serine (PerkinElmer) for 6 h at 37 °C, at the end of the 48 h palmitate treatment. For the NBD–Cer assay, total lipid was extracted with 10 mM chloroform/methanol/EDTA in PBS [1:1:0.75, by vol.] following washing in PBS supplemented with 10 mM EDTA. The organic phase was removed, dried down under nitrogen and re-dissolved in 30 μl of chloroform/methanol [1:1 (v/v)] and run on a HPTLC (high-performance TLC) plate (Merck) in butanol/acetic acid/water [3:1:1, by vol.] as a solvent system with appropriate lipid standards for SM, GlcCer and Cer. HPTLC plates were imaged on a UV light box within a Bio-Rad ChemiDoc XRS imager. For the [^{3}H]serine assay, total lipid was extracted with chloroform/methanol [2:1 (v/v)], dried down under nitrogen, then re-dissolved in 50 μl of choloroform/methanol [2:1 (w/w)] to be run on a TLC plate. A portion of total lipid extract (2.5 μl) was combined with 6 ml of scintillation fluid (Ultima Gold, PerkinElmer) for later quantification before spotting the remainder on the TLC plate (Whatman) with the aforementioned lipid standards. The plate was run on a two-front system: the first solvent system was chloroform/methanol/acetic acid [190:9:1, by vol.], the second was diethyl ether/acetic acid [100:1 (v/v)]. Areas on the TLC plate corresponding to the lipid standard Cer were scraped, combined with 6 ml of scintillation fluid and quantified on a β-counter (Beckman Coulter).

ROS (reactive oxygen species) assay

The levels of intracellular ROS were measured in MIN6 and PR cells by their ability to convert the acetyl ester CM-H_2DCFDA into a fluorescent product (excitation/emission, 485 nm/520 nm). Cells plated in 24-well plates and pre-treated with palmitate or oleate (48 h) or 1 mM alloxan as a positive control (10 min), were washed once with warm HBSS (Hanks buffered salt solution). The medium was replaced with 0.8 ml of HBSS containing 1 μM CM-H_2DCFDA and incubated at 37 °C for 30 min. The plate was placed on ice, all wells were washed with cold HBSS and then scraped in 0.5 ml of HBSS where 200 μl of cell suspension was loaded into a black uncoated 96-well plate to be read on a fluorescence plate reader (FluoStar OPTIMA, BMG Lab Technologies). The remainder of each sample was assayed for total protein (BCA protein assay kit), to correct for total cellular content per well.

Lipid profiling with MS

Following chronic palmitate treatment, lipids were extracted from MIN6 cell homogenates (two 15 cm^2 dishes per condition) using chloroform/methanol [2:1 (v/v)] or individual sucrose fractions using chloroform/methanol [1:2 (v/v)] and including 100 pmol of Cer $C_{17:0}$, GlcCer $C_{16:0(d3)}$, LacCer $C_{16:0(d3)}$, THC $C_{17:0}$ (Matreya), PC (13:0/13:0), PG (phosphatidylglycerol) (17:0/17:0), PE (phosphatidylethanolamine) (17:0/17:0), PS (phosphatidylserine) (17:0/17:0) and SM $C_{12:0}$ (Avanti Polar Lipids), 500 pmol of DAG (diacylglycerol) (15:0/15:0) and TAG (triacylglycerol) (17:0/17:0/17:0) (Sigma–Aldrich), and 1000 pmol of CE (cholesteryl ester) $C_{18:0(d6)}$ (CDN Isotopes) as internal standards. Analysis was performed by ESI (electrospray ionization)-tandem MS using a PE Sciex API 4000 Q/TRAP mass spectrometer with a turbo-ionspray source and Analyst 1.5 data system. Prior liquid chromatographic separation was performed on a Zorbax C_{18}, 1.8 μm, 50 mm × 2.1 mm column at 300 μl/min using the following gradient conditions for all lipid species except DAGs and TAGs: 100 % A to 0 % A over 8.0 min followed by 2.5 min at 0 % A, a return to 100 % A over 0.5 min then 3.0 min at 100 % A prior to the next injection. Solvent A and B consisted of tetrahydrofuran/methanol/water in the ratios 30:20:50 and 75:20:5 respectively, both containing 10 mM ammonium formate. Chromatography of DAG and TAG species was performed in isocratic mode using 85 % A and 15 % B at 100 μl/min. Quantification of individual lipid species was performed using scheduled multiple-reaction monitoring in positive-ion mode. Individual lipid species monitored were the major species (greater than 1 % of total) identified in human plasma. Multiple-reaction monitoring experiments were based on product ion of *m/z* 264 [sphingosine-H_2O]$^+$ for Cer, GlcCer, LacCer and THC, *m/z* 184 [PC]$^+$ for SM and PC, *m/z* 369 [cholesterol-H_2O]$^+$ for CE and NL (neutral loss) of 141 Da for PE, 185 Da for PS, 277 Da for PI (phosphatidylinositol) and 189 Da for PG. Product ions for DAGs and TAGs were based on the neutral loss of one FA from the [M^+–NH_4]$^+$ ion. Each ion pair was monitored for 10–50 ms with a resolution of 0.7 atomic mass unit at half-peak height and averaged from continuous scans over the elution period. Lipid concentrations were calculated by relating the peak area of each species to the peak area of the corresponding internal standard. PI species were related to the PE internal standard. For DAG and TAG species containing two or three of the same FA used as a NL, the signal response was corrected by dividing by the number of copies of the FA. Total lipids of each class were determined by summing the individual lipid species.

Please note that the MS analysis used in the present study does not distinguish between GlcCer and galactosylceramide, but the former predominates in MIN6 cells as assessed by TLC analyses (2.3 ± 0.2-fold, $n = 3$) and is the only glycosylated Cer generated by GCS. For simplicity we therefore refer to this species as GlcCer.

VSVG (vesicular stomatis viral glycoprotein temperature-sensitive mutant)–GFP trafficking assay

MIN6 cells were nucleofected with VSVG [18]. Where indicated the cells were also co-transfected with equimolar concentrations of the GCS construct, before plating on to glass coverslips and treatment with chronic palmitate or control medium. After overnight treatment at 40 °C to retain the VSVG in the ER, trafficking was commenced by switching cells to the permissive temperature of 32 °C, and addition of 20 μM cycloheximide to prevent new VSVG synthesis. Scoring of coverslips using confocal images involved grading the co-localization of VSVG with the Golgi as it moves from the diffuse ER region to the distinct perinuclear structure of the Golgi. The scale was from 1 (being all ER, no Golgi) to 5 (being all Golgi, no ER). A grading of 3 corresponded to equal intensities of VSVG in the ER and Golgi (half ER, half Golgi), 2 indicated mostly ER with some Golgi co-localization and 4 meant some ER, but mostly Golgi positioning. The scoring was performed by two independent observers.

Immunoblotting

Protein lysates were prepared and protein content was equalized after quantification using a BCA protein assay (Pierce) before undergoing Western blot analysis and detection of ER stress induction as described previously [9]. Antibodies used included those against GADD153 (growth-arrest and DNA-damage-inducible protein 153) (CHOP, Santa Cruz Biotechnology), β-actin (Sigma–Aldrich) and GM130 (*cis*-Golgi matrix protein of 130 kDa) (BD Transduction Laboratories). Quantification of Western blot films was performed using ImageJ [36].

Statistical analysis

All results are presented as means + S.E.M. Data sets were subject to a one-way ANOVA (with Bonferonni or Dunnett's multiple comparison post-tests), or paired Student's *t* tests. Non-parametric analysis was undertaken using the Mann–Whitney test.

RESULTS

Alterations in sphingolipid metabolites are associated with palmitate-induced apoptosis in MIN6 cells.

In principle, the toxic lipid species responsible for lipo-apoptosis in β-cells might comprise a member of the neutral lipid, phospholipid or sphingolipid classes. To address this in an unbiased fashion we have used MS to undertake a comprehensive screen of alterations in major lipid classes during lipotoxicity. We used as our model the well-differentiated MIN6 cell line under conditions in which mild apoptosis and ER stress are induced over 48 h by palmitate, but not oleate [9,11,34]. We used FA pre-coupled to BSA at a 3:1 molar ratio, which is in the moderately elevated physiological range, and corresponds to a free FA concentration in the low micromolar range [37]. The degree, timing and selectivity of apoptosis for saturated FAs in this model are broadly in keeping with findings using primary mouse and human islets [10,11]. In contrast, rat islets and cell lines are generally more sensitive to FA-induced apoptosis, probably

Table 1 Neutral lipid content (TAG, DAG and CE) in whole MIN6 cell lysates following chronic palmitate treatment

Chronic palmitate treatment of MIN6 cells (see the Experimental section) comprised culture for 48 h in 0.4 mM palmitate (complexed to 0.92 g/100 ml BSA) or control medium (BSA alone). Lipids were extracted and analysed by MS.

	Control			Palmitate		
Measurement	TAG	DAG	CE	TAG	DAG	CE
Mass (nmol/mg)	8.95 ± 1.2	6.78 ± 0.99	44.0 ± 7.3	14.3 ± 1.2*	10.0 ± 1.1*	39.5 ± 4.0
Percentage saturated	49.4 ± 1.4	38.3 ± 1.2	28.5 ± 1.0	62.6 ± 1.0***	56.4 ± 1.0***	33.0 ± 0.8**
Percentage of $C_{16:0}$	36.8 ± 2.0	21.4 ± 0.7	20.7 ± 1.0	50.6 ± 1.2**	41.9 ± 1.2***	24.4 ± 0.7**

*$P < 0.05$, **$P < 0.01$, ***$P < 0.001$, using Student's paired t tests compared with the corresponding control.

because they poorly express stearoyl-CoA desaturase [38], which is critical for detoxifying saturated FAs [11] or for maintaining a critical pool of unsaturated lipid [13].

When neutral lipids were assayed following palmitate pre-treatment, the total masses of TAG and DAG were increased by approx. 70 % and 40 % respectively, whereas overall CE was not significantly altered (Table 1). As shown previously using rat INS-1 β-cells [39,40] there was a high proportion of saturated FAs, especially palmitate ($C_{16:0}$), present as TAG side chains in MIN6 cells under control conditions, but in our hands these proportions were only relatively modestly increased by chronic exposure to palmitate. In contrast, the percentage of total saturated FA in DAG was markedly increased under these conditions, and the proportion of $C_{16:0}$ was approximately doubled. Remodelling of CE side chains was minimal (Table 1).

Of the phospholipid classes, PG and PS masses were unaltered by palmitate pre-treatment, but there were slight decreases in PI and increases in PC (Figure 1A). These changes are unlikely to play a causative role in lipo-apoptosis since they were also observed in PR cells, a subpool of MIN6 cells that have been selected for up-regulation of stearoyl-CoA desaturase and thus do not undergo apoptosis when exposed to palmitate [11]. The biggest fold increases occurred in PE, 55 % in MIN6 cells and 36 % in PR cells, although the latter did not reach statistical significance. When saturation indices were calculated for all of these phospholipids (results not shown), only PC was altered significantly upon exposure to palmitate (Figure 1B). Although this increase was not always so pronounced in subsequent experiments (see below), the fact that it was significantly smaller in the PR cells (although still elevated) raises the possibility that PC saturation might be linked mechanistically to lipo-apoptosis.

The major alterations that we (consistently) observed following chronic palmitate exposure were in the sphingolipid class, although the overall masses of both Cer and SM were unchanged (Figure 2A). In contrast, the glycosylated derivatives GlcCer, LacCer and THC were all significantly elevated, and to a greater extent in MIN6 cells compared with PR cells (Figure 2A). This was most apparent in GlcCer (the direct metabolite of Cer), which was increased by 75 % in MIN6 cells, but not significantly in PR cells. When Cer mass was analysed in greater detail, abundant species were unchanged in both MIN6 and PR cells in response to palmitate (Figure 2B). All major species of GlcCer, including long-chain and unsaturated variants, were increased by palmitate in MIN6 cells (Figure 2C). These effects were less pronounced in PR cells. The results for SM (Figure 2D) were more complex. Although $C_{18:0}$ SM was significantly enhanced by palmitate (in MIN6 cells only) the $C_{24:0}$ and $C_{24:1}$ species were diminished in MIN6 cells (and to a broadly similar extent in PR cells). These decreases in SM were not accompanied by elevations in the corresponding Cer species, so are unlikely to have arisen as a result of enhanced activity of sphingomyelinase.

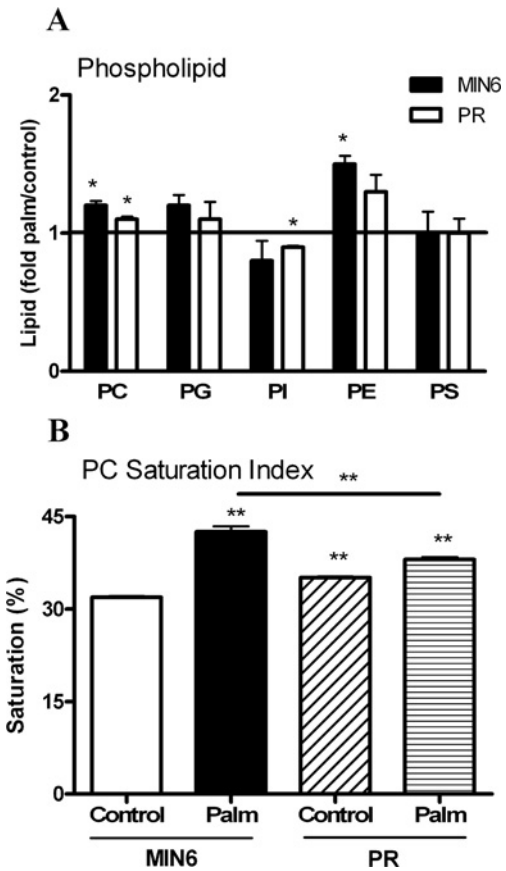

Figure 1 Effects of chronic palmitate treatment on phospholipid mass and saturation in MIN6 and PR cells

All cells underwent chronic palmitate treatment involving culture for 48 h in medium containing FA pre-coupled to BSA at a 3:1 molar ratio or BSA alone (see the Experimental section). Lipids were extracted and analysed by MS. (**A**) Total mass of phospholipids PC, PG, PI, PE and PS, expressed as the effect of palmitate relative to the corresponding BSA-treated control, from three independent experiments. *$P < 0.05$, using one-way ANOVA with Dunnett's post-tests comparing each treatment with the control group. (**B**) Saturation index of PC, calculated from the mass of species with saturated side chains as a percentage of the mass of all species. **$P < 0.01$, using Student's paired t test compared with the corresponding control or as indicated.

Enhanced flux through Cer contributes to ER stress and apoptosis

The above results suggest that flux through sphingolipid metabolites is increased under these conditions, resulting in steady-state accumulation of glycosylated derivates (especially GlcCer) rather than Cer itself. To assess flux more directly we pulsed MIN6 cells for 6 h with [^{3}H]serine, which is incorporated into Cer via

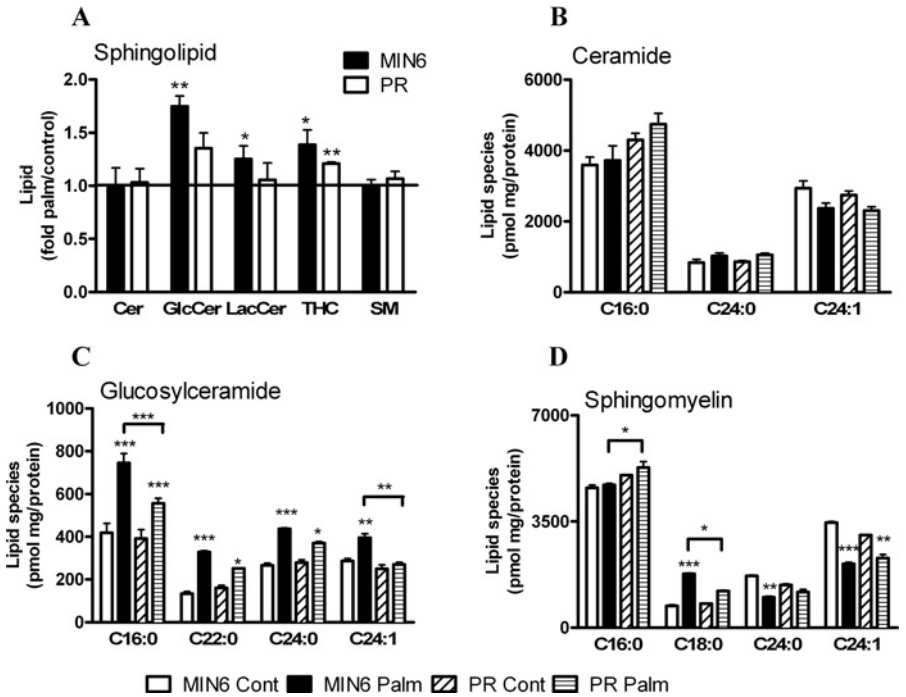

Figure 2 Effects of chronic palmitate treatment on sphingolipids in MIN6 and PR cells

Cells were treated chronically with palmitate, and then total lipids were extracted and analysed by MS as described in the legend to Figure 1. (**A**) Total mass of sphingolipids Cer, GlcCer, LacCer, THC and SM, expressed as the effect of palmitate relative to the corresponding BSA-treated control. Results are from three independent experiments. $^{*}P < 0.05$, $^{**}P < 0.01$, using one-way ANOVA with Dunnett's post-tests comparing each treatment with control group. (**B**–**D**) Mass of individual lipid species in Cer, GlcCer and SM, carbon side-chain lengths are as indicated ($n = 3$). $^{*}P < 0.05$, $^{**}P < 0.01$, $^{***}P < 0.001$, using one-way ANOVA with Bonferroni post-tests comparing each treatment with the control group, except where indicated.

SPT1 (serine palmitoyltransferase 1) in the first step of *de novo* synthesis. Labelling of Cer was significantly increased following palmitate pre-treatment, consistent with an increase in flux (Figure 3A). This was abolished by the SPT1 inhibitor cycloserine (0.5 mM). Several prior studies have demonstrated that inhibiting the synthesis of Cer diminishes apoptosis in lipotoxic β-cells [6,27–29]. However, this has not always been observed [30–32], and involvement of Cer metabolism in ER stress in β-cell lipotoxicity has only been addressed once previously [32]. In the present study we confirm that the SPT1 inhibitor myriocin (100 nM) inhibits the activation of caspase 3 due to palmitate in our model (Figure 3B). Importantly, this was accompanied by a reduced induction of the ER stress marker CHOP (Figure 3C).

Palmitate-induced alterations in sphingolipid metabolites are not secondary to ER stress

ER stress can itself lead to remodelling of cellular lipids [41,42]. We therefore sought to determine whether the observed changes in phospholipids and sphingolipids were secondary to ER stress. PBA, a chemical chaperone [16], was used to alleviate ER stress in the presence of palmitate, as witnessed by the decreased expression of the terminal ER stress protein CHOP (Supplementary Figure S1 at http://www.BiochemJ.org/bj/435/bj4350267add.htm). Conversely, we employed thapsigargin and tunicamycin to induce ER stress. Thapsigargin, an inhibitor of the ER calcium pump, depletes ER calcium stores and thereby compromises ER enzyme function. This compound is a strong ER stress inducer in our model [18]. Tunicamycin, which disrupts protein N-glycosylation at the ER and therefore protein export to the Golgi, also induces ER stress as a result of protein backlog in the organelle [9,18]. Importantly, co-treatment with PBA did not abolish the effects of palmitate on total PE, GlcCer or SM (Figure 4), indicating that these effects were not secondary to ER stress. Likewise, responses due to palmitate on these lipids were not recapitulated by thapsigargin or tunicamycin treatment. Moreover, the increase in PC saturation due to palmitate (statistically significant but smaller than observed in Figure 1B) was actually further elevated with PBA (Figure 4B). PC saturation was increased by tunicamycin but not thapsigargin, so it cannot simply be a consequence of ER stress. Importantly, none of these pharmacological interventions altered Cer mass (Figure 4C). Taken together these results illustrate that the induction of ER stress itself is neither necessary for the observed effects of palmitate on these lipids, nor sufficient to reproduce them.

Overexpression of GCS protects MIN6 cells from lipo-apoptosis, terminal ER stress and from the palmitate-induced delay in protein trafficking

Given the marked increase in GlcCer in MIN6 cells following chronic palmitate treatment (Figure 2A), we postulated that this metabolite could contribute to cytotoxicity as observed previously in other cell types [33,43]. We therefore sought to determine whether apoptosis would be increased by enhancing GlcCer mass even further by overexpression of GCS, which catalyses the conversion of Cer into GlcCer. Conversely, if Cer rather than GlcCer were the toxic species, this manipulation would be predicted to decrease apoptosis. Functional overexpression was confirmed by increases in both the endogenous mass ratio of GlcCer to Cer (Figure 5A), and the conversion of exogenous NBD–Cer into NBD–GlcCer from (Supplementary Figure S2 at http://www.BiochemJ.org/bj/435/bj4350267add.htm). GCS overexpresson decreased both CHOP induction due to palmitate

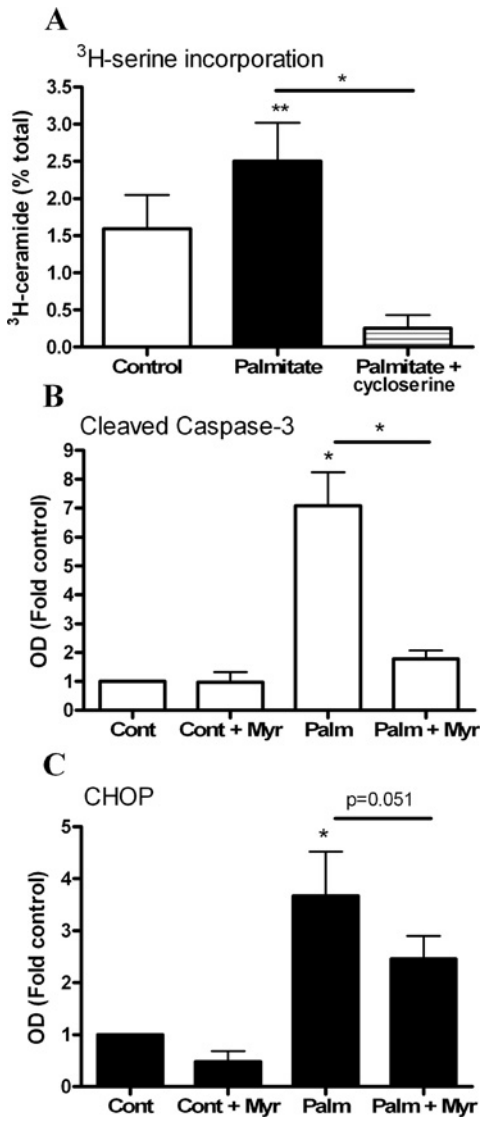

Figure 3 Effects of inhibition of SPTI by cycloserine or myriocin (Myr) in MIN6 cells on Cer synthesis, apoptosis and ER stress

(**A**) Cells were treated chronically with 0.4 mM palmitate pre-coupled to 0.9 g/100 ml BSA (molar ratio 3:1) $\pm$ cycloserine and labelled for the final 6 h with 40 μCi of [^{3}H]serine. Total lipids were extracted and analysed by TLC. Data are presented as the incorporation of [^{3}H]serine into Cer over 6 h, expressed as a percentage of total ^{3}H-labelled lipid. $^*P < 0.05$, $^{**}P < 0.01$, using paired Student's *t* test ($n = 4$ for all except, $n = 3$ for the palmitate + cycloserine condition). (**B**) Total protein lysates were also prepared for analysis via immunoblotting (see the Experimental section) following chronic palmitate treatment $\pm$ myriocin. Quantification of cleaved caspase 3 protein content (ImageJ software), from three independent Western blots. $^*P < 0.05$, using Student's paired *t* test. (**C**) Quantification of CHOP content (ImageJ software), from three independent Western blots. $^*P < 0.05$, using Student's paired *t* test.

(Figure 5B) and lipo-apoptosis in MIN6 cells (Figure 5C). These results therefore implicate Cer rather than GlcCer as the toxic metabolite. We also confirmed that the protection afforded by overexpression of GCS was not secondary to an indirect effect on the PC saturation index. In this series of experiments there was a modest increase in PC saturation due to palmitate, which was independent of GCS overexpression (Figure 5D). Likewise the increase in overall PE mass due to palmitate was not altered under these conditions (Figure 5E).

We previously reported that chronic palmitate treatment of MIN6 cells retards ER-to-Golgi protein traffic as measured using a VSVG reporter protein [18]. In this assay VSVG is excluded from the Golgi (stained with anti-GM130) at 0 min (Supplementary Figure S3 at http://www.BiochemJ.org/bj/435/bj4350267add.htm). At 20 min after the switch to the permissive temperature of 32 °C, most of the VSVG had reached the Golgi. Cells treated with chronic palmitate showed a clear delay in trafficking at 20 min, with a significant amount of VSVG retained in the diffuse ER region (Supplementary Figure S3). However, in palmitate-treated MIN6 cells that were co-transfected with the GCS construct, VSVG localization appeared similar to that of controls. Figure 5(F) shows a histogram of the average scores of individual cells, according to localization of the VSVG protein. Palmitate treatment significantly reduced the average score, indicative of lesser Golgi localization. Cells co-expressing VSVG and GCS in the presence of palmitate produced very similar co-localization scores to those of control cells. These changes in individual cellular VSVG trafficking events confirm that GCS overexpression rescues the trafficking defect due to palmitate treatment.

ROS generation does not correlate with lipotoxicity in MIN6 cells

Oxidative stress and ER stress are potentially linked in β-cell lipotoxicity [14,17], and in other cell types the generation of ROS and Cer can occur either up- or down-stream of each other depending on the circumstances [44]. We therefore measured ROS induction in our model. As shown in Figure 6, neither palmitate nor oleate significantly increased ROS in MIN6 cells. Basal ROS generation was slightly higher in PR cells than MIN6 cells, but not further increased following treatment with either FA. The robust increase with alloxan, which is specifically transported into β-cells and generates intracellular ROS [45], serves as a positive control.

DISCUSSION

The β-cell failure that underlies development of Type 2 diabetes has been linked to the inability of susceptible β-cells to handle nutrient overload, particularly in response to elevated circulating FAs [1,4]. Hence the mechanisms underlying β-cell lipotoxicity are under active investigation. Attention has focused on the capacity of saturated FAs to induce ER stress [8–10] and the implications of this for the enhanced apoptosis and loss of β-cell mass that contributes to Type 2 diabetes. Older literature links β-cell apoptosis to Cer accumulation [6,27–29], although this has not been without controversy [30–32]. Moreover, the relevance of these findings to ER stress in β-cells is unclear, and indeed a broader body of work would point to the potential involvement of candidate lipids other than Cer [20–22].

Our current goal was therefore to conduct an unbiased and comprehensive screen of all major lipid classes in order to identify the metabolic alterations that accompany ER stress and apoptosis when β-cells are chronically exposed to saturated FAs. We now demonstrate that mass alterations in major lipid classes are remarkably modest under these conditions. For example, total TAG was increased by less than two-thirds in MIN6 cells chronically exposed to palmitate, and overall incorporation of $C_{16:0}$ side chains was limited to approx. 50 %. This contrasts with a study using rat INS-1 cells where TAG mass was augmented severalfold, and overall $C_{16:0}$ content reached >90 % of the total TAG pool following palmitate pre-treatment [39]. Our current findings are, however, in broad agreement with previous tracer analyses [11], which suggested that TAG deposition was not implicated in apoptosis in our model since similar alterations in TAG were observed in both parental MIN6 cells and PR cells

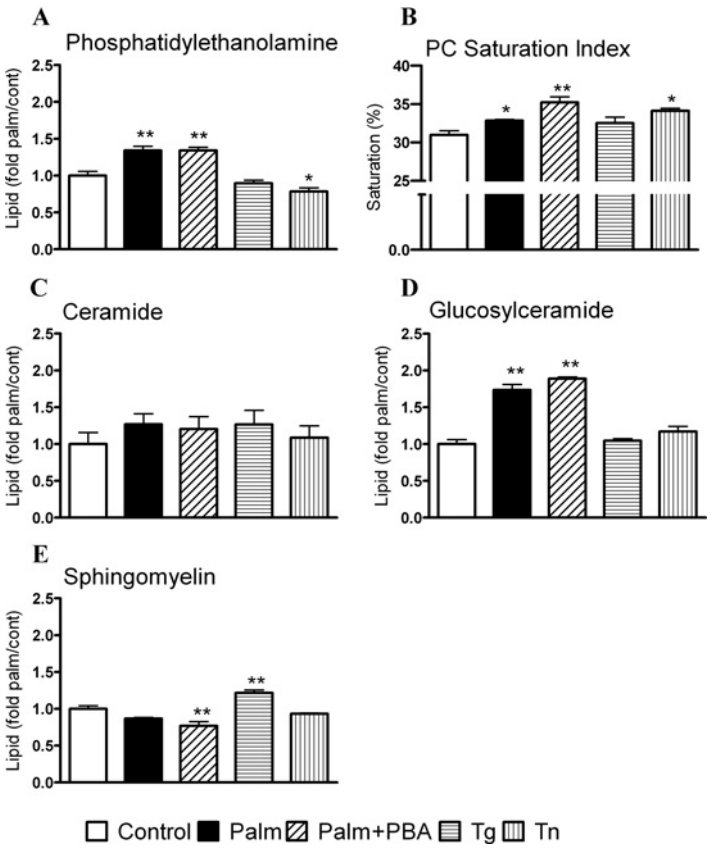

Figure 4 Alterations in lipid classes due to palmitate treatment are not secondary to ER stress

MIN6 cells were treated for 48 h, with Palm (0.4 mM palmitate with 0.92 g/100 ml BSA) ± PBA at 5 mM, or for 24 h with thapsigargin (Tg) at 50 nM or tunicamycin (Tn) at 2 μM compared with control (0.92 % BSA). Lipid extracts were analysed by MS and results were corrected with PS as a loading control, and are expressed relative to the corresponding control treatment groups. (**A**) PE mass, (**B**) PC saturation index, (**C**) Cer mass, (**D**) GlcCer mass and (**E**) SM mass. Results are from three independent experiments. $^{*}P < 0.05$, $^{**}P < 0.01$, using one-way ANOVA with Dunnett's post-tests comparing each treatment with the control group.

[11]. This is also consistent with the conclusions of other studies using both β-cells and other cellular models [7,46]. We have also demonstrated previously that inhibition of CE formation did not impact on apoptosis [11]. For these reasons we believe that metabolism of TAG and CE is unlikely to exert major effects on ER stress and lipo-apotosis in this model. On the other hand, we show in the present study that increases in the saturation of DAG did occur under these conditions, albeit with only a modest increase in overall DAG mass. Therefore we cannot formally exclude the possibility that this might contribute to apoptosis. The underlying mechanism, however, would be obscure because saturated DAG species are not likely to exert any function on signalling enzymes such as protein kinase C [47].

The results of the present study further demonstrate that lipotoxic β-cells undergo reproducible alterations in sphingolipid profiles, in particular an enhancement of GlcCer mass. These changes were neither abolished by co-treatment with the chaperone PBA, nor reproduced by pharmacological inducers of ER stress, indicating that they are primary consequences of chronic exposure to palmitate and not the result of ER stress itself. We do not exclude, however, the possibility that strong ER stress induced by high doses of pharmacological agents might activate sphingomyelinase and thereby generate Cer, as proposed previously [48]. We also demonstrated that palmitate pre-treatment promotes an enhanced flux through Cer synthetic pathways, which is manifest as an accumulation in GlcCer, but not in the immediate precursor, Cer. It is noteworthy that most prior evidence of a role for Cer in β-cell lipotoxicity was based on tracer measurements [27,28], which are also indicative of flux rather than steady levels. In previous studies where Cer mass was actually determined there was little change after chronic palmitate unless glucose was also elevated [31,49]. Likewise Cer was modestly elevated in islets isolated from a genetically diabetic mouse model, but only late in the progression of the disease [50,51]. This is entirely consistent with the results of the present study.

In keeping with many [6,27–29], but not all, prior studies [30–32], we also confirmed that inhibition of *de novo* Cer synthesis partially ablated the induction of β-cell apoptotic markers in response to FA. Our results also link Cer metabolism to lipotoxic ER stress in β-cells for the first time, although this connection has been made using other experimental systems [25,52]. However, the use of proximal inhibitors of *de novo* Cer synthesis does not allow for distinguishing between lipotoxicity due to Cer itself compared with putative effects of its downstream metabolites. We have now addressed this by demonstrating that enhancing the conversion of Cer into GlcCer, by overexpression of GCS, protects against apoptosis, ER stress and defective protein trafficking. These results not only strengthen the conceptual links between these processes, but also implicate Cer, and not GlcCer, as the metabolite that precipitates them. That Cer might play such a role in the absence of any increase in its overall cellular mass perhaps implies that a putative alteration in specific subcellular compartments might be important. The topology of

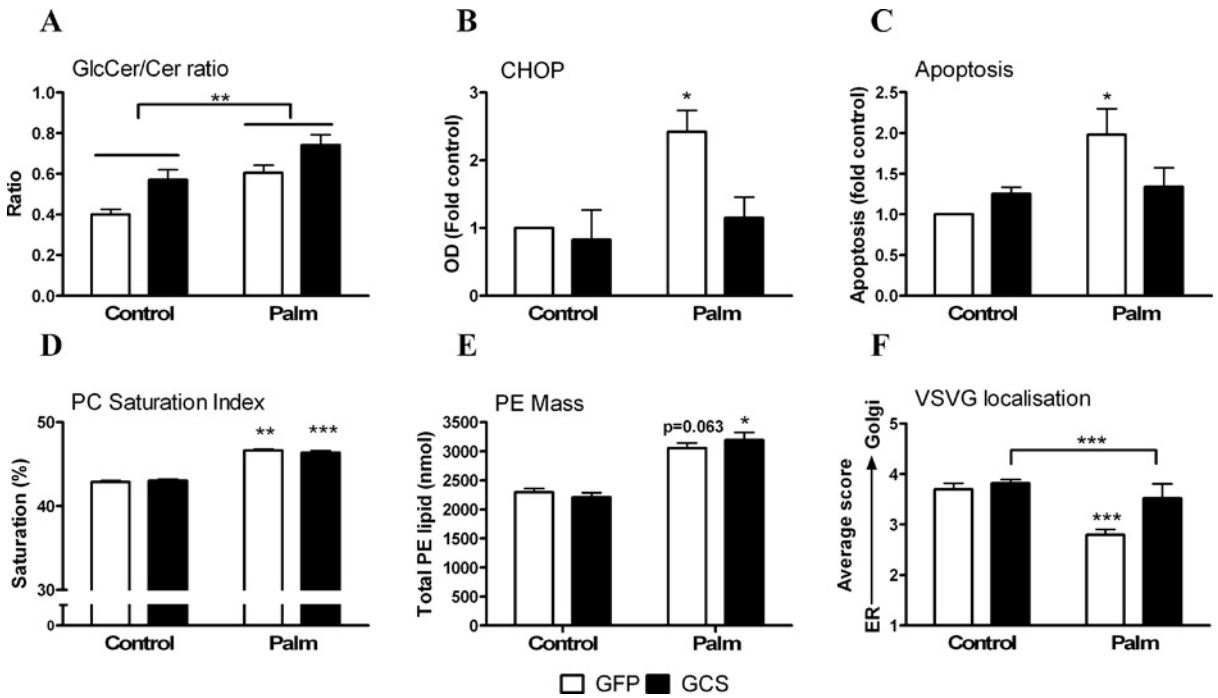

Figure 5 Overexpression of GCS protects MIN6 cells against apoptosis, ER stress and defective protein trafficking due to chronic palmitate treatment

MIN6 cells were transfected with GFP or GCS (see the Experimental section) and then treated for 48 h with 0.4 mM palmitate with 0.92 g/100 ml BSA or 0.92 g/100 ml BSA alone. (**A**) Total cellular ratio of GlcCer to Cer. Lipid extracts were analysed by MS. $^{**}P < 0.01$, using Student's paired *t* test. (**B**) Densitometric analysis of CHOP protein expression, normalized to the control GFP value. $^{*}P < 0.05$ using one-way ANOVA with Bonferroni post-tests. (**C**) Apoptosis measured using a histone-bound DNA fragment ELISA, normalized to the control GFP value. $^{*}P < 0.05$ using one-way ANOVA with Bonferroni post-tests. (**D**) PC saturation index. $^{**}P < 0.01$, $^{***}P < 0.001$, using Student's paired *t* test for palmitate treatment compared with the corresponding control. (**E**) PE mass. $^{*}P < 0.05$, using Student's paired *t* test for palmitate treatment compared with the corresponding control. (**F**) MIN6 cell average scores of VSVG localization from a scale from 1 to 5 (see the Experimental section) within each treatment group. Cells were transfected with VSVG (as well as GCS where indicated), pre-treated with palmitate, incubated overnight at 40 °C to trap VSVG in the ER and then switched to 32 °C to allow trafficking of VSVG to the Golgi over 20 min. At least 50 cells from each group were scored by two independent observers . $^{***}P < 0.001$, using a Mann–Whitney test. All results are from three to four independent experiments. Palm, palmitate.

sphingolipid metabolism, however, is complex and much further experimentation will be required to test exactly how and where it potentially intersects with the protein trafficking machinery to modulate ER stress.

In direct contrast with our results, myriocin did not inhibit CHOP induction by palmitate in another recent study using MIN6 cells [32]. However, the authors of this study used a molar ratio of palmitate to BSA that is approximately double that of the present study. Free FA concentrations are likely to be considerably higher under those conditions [37], perhaps triggering alternative mechanisms of lipotoxicity that predominate over the ER stress that is causally implicated in our milder model [9,16]. One such mechanism might be ROS generation, which appears to be highly dependent on the FA to BSA molar ratio to which β-cells are exposed. In contrast with the findings of the present study, and those of Moore et al. [53], which employed ratios of 3 and 5 respectively, pre-treatment of β-cells at FA/BSA ratios of 6 and above has been reported to promote modest but significant increases in markers of oxidative stress [13,54–57]. In several instances, however, these were induced by oleate as well as palmitate [55–57], and so are more probably implicated in the development of β-cell secretory dysfunction, which is induced by both these FAs [34,58], as opposed to apoptosis, which is more sensitive to saturated FAs [6–10].

The present study also characterized the alterations in phospholipid profiles that accompany β-cell lipotoxicity. The most pronounced changes, in both MIN6 and PR cells, were increases in total PE mass, although the PE saturation index was unaltered in either cell type. In contrast we did observe a

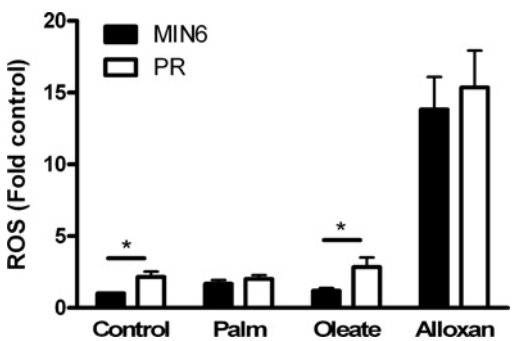

Figure 6 Effects of FA pre-treatment on ROS levels in MIN6 and PR cells

Cells were treated for 48 h with FA or BSA alone (control) as described in the legend to Figure 1. ROS were measured following palmitate or oleate pre-treatment via oxidation of the acetyl ester CM-H_2DCFDA to a fluorescent product. Values are the mean fold control (fluorescence/total protein) + S.E.M. for five independent experiments. $^{*}P < 0.05$, using Student's paired *t* test.

consistent increase in PC saturation. By analogy with findings using yeast [21], CHO (Chinese-hamster ovary) cells [20] and HeLa cells [21,22], this might potentially contribute to ER stress. Although we do not completely exclude this possibility, for a number of reasons we believe this explanation is less likely than the alterations in sphingolipid metabolism described above. First, both baseline PC saturation, and the degree to which it increased following palmitate treatment, varied somewhat between different study groups but never exceeded 50 %. This is in contrast

with studies in yeast and HeLa cells where ER stress was accompanied by incorporation of more than 60 % saturated FAs into phospholipids [21,22]. Secondly, the increases we observed were not diminished by overexpression of GCS, whereas this intervention did protect against apoptosis, ER stress and defective trafficking, consistent with enhanced Cer metabolism to GlcCer. Finally, mechanisms established using other cellular models might not be relevant to β-cells since the latter have clearly been shown to be remarkably resistant to a lipotoxic challenge as compared with other peripheral tissues [50].

In summary, the results of the present study provide evidence that metabolites of sphingolipids, rather than of neutral lipids or phospholipids, are likely to be involved in the development of ER stress and lipo-apoptosis in β-cells. Our data also lend support to the idea that protein overload, secondary to reductions in ER-to-Golgi protein trafficking, contributes to the induction of ER stress in β-cells that is triggered intrinsically by chronic exposure to palmitate, and which is potentially implicated in the β-cell failure of Type 2 diabetes.

AUTHOR CONTRIBUTION

Ebru Boslem performed most of the experimental work and wrote the first draft of the manuscript. Gemma MacIntosh and Clarissa Bartley performed some experimental work. Amanda Preston and Anna Karina Busch helped to develop and perform some of the experimental work. Maria Fuller and Ross Laybutt oversaw some of the experimental work and helped to review the manuscript prior to submission. Peter Meikle helped to develop and oversaw some of the experimental work and helped to review the manuscript prior to submission. Trevor Biden initiated and oversaw the study and revised the manuscript. All authors approved the manuscript.

ACKNOWLEDGEMENTS

We thank Professor David James (Garvan Institute of Medical Research, Sydney, Australia) for the gift of the VSVG construct, originally from Professor J. Lippincott-Schwartz. We also thank Dr Will Hughes for confocal microscopy training.

FUNDING

This work was supported by the National Heath and Medical Research Council of Australia project grant (to T.J.B. and D.R.L.), Research Fellowships (to T.J.B. and P.J.M.), and a postgraduate scholarship (to E.B.).

REFERENCES

1 Kahn, S. E., Hull, R. L. and Utzschneider, K. M. (2006) Mechanisms linking obesity to insulin resistance and type 2 diabetes. Nature **444**, 840–846
2 Prentki, M. and Nolan, C. J. (2006) Islet β-cell failure in type 2 diabetes. J. Clin. Invest. **116**, 1802–1812
3 Muoio, D. M. and Newgard, C. B. (2008) Mechanisms of disease: molecular and metabolic mechanisms of insulin resistance and β-cell failure in type 2 diabetes. Nat. Rev. Mol. Cell Biol. **9**, 193–205
4 Lewis, G. F., Carpentier, A., Adeli, K. and Giacca, A. (2002) Disordered fat storage and mobilization in the pathogenesis of insulin resistance and type 2 diabetes. Endocr. Rev. **23**, 201–229
5 Newsholme, P., Keane, D., Welters, H. J. and Morgan, N. G. (2007) Life and death decisions of the pancreatic β-cell: the role of fatty acids. Clin. Sci. **112**, 27–42
6 Maedler, K., Spinas, G. A., Dyntar, D., Moritz, W., Kaiser, N. and Donath, M. Y. (2001) Distinct effects of saturated and monounsaturated fatty acids on β-cell turnover and function. Diabetes **50**, 69–76
7 Cnop, M., Hannaert, J. C., Hoorens, A., Eizirik, D. L. and Pipeleers, D. G. (2001) Inverse relationship between cytotoxicity of free fatty acids in pancreatic islet cells and cellular triglyceride accumulation. Diabetes **50**, 1771–1777
8 Karaskov, E., Scott, C., Zhang, L., Teodoro, T., Ravazzola, M. and Volchuk, A. (2006) Chronic palmitate but not oleate exposure induces endoplasmic reticulum stress, which may contribute to INS-1 pancreatic β-cell apoptosis. Endocrinology **147**, 3398–3407
9 Laybutt, D. R., Preston, A. M., Akerfeldt, M. C., Kench, J. G., Busch, A. K., Biankin, A. V. and Biden, T. J. (2007) Endoplasmic reticulum stress contributes to β-cell apoptosis in type 2 diabetes. Diabetologia **50**, 752–763
10 Cunha, D. A., Hekerman, P., Ladriere, L., Bazarra-Castro, A., Ortis, F., Wakeham, M. C., Moore, F., Rasschaert, J., Cardozo, A. K., Bellomo, E. et al. (2008) Initiation and execution of lipotoxic ER stress in pancreatic β-cells. J. Cell Sci. **121**, 2308–2318
11 Busch, A. K., Gurisik, E., Cordery, D. V., Sudlow, M., Denyer, G. S., Laybutt, D. R., Hughes, W. E. and Biden, T. J. (2005) Increased fatty acid desaturation and enhanced expression of stearoyl coenzyme A desaturase protects pancreatic β-cells from lipoapoptosis. Diabetes **54**, 2917–2924
12 Dhayal, S. and Morgan, N. G. (2010) Pharmacological characterisation of the cytoprotective effects of polyunsaturated fatty acids in insulin-secreting BRIN-BD11 cells. Br. J. Pharmacol., doi: 10.1111/j.1476–5381.2010.01145.x
13 Keane, D. C., Takahashi, H. K., Dhayal, S., Morgan, N. G., Curi, R. and Newsholme, P. (2011) Arachidonic acid actions on functional integrity and attenuation of the negative effects of palmitic acid in a clonal pancreatic β-cell line. Clin. Sci. **120**, 195–206
14 Scheuner, D. and Kaufman, R. J. (2008) The unfolded protein response: a pathway that links insulin demand with β-cell failure and diabetes. Endocr. Rev. **29**, 317–333
15 Eizirik, D. L., Cardozo, A. K. and Cnop, M. (2008) The role for endoplasmic reticulum stress in diabetes mellitus. Endocr. Rev. **29**, 42–61
16 Akerfeldt, M. C., Howes, J., Chan, J. Y., Stevens, V. A., Boubenna, N., McGuire, H. M., King, C., Biden, T. J. and Laybutt, D. R. (2008) Cytokine-induced β-cell death is independent of endoplasmic reticulum stress signaling. Diabetes **57**, 3034–3044
17 Song, B., Scheuner, D., Ron, D., Pennathur, S. and Kaufman, R. J. (2008) CHOP deletion reduces oxidative stress, improves β-cell function, and promotes cell survival in multiple mouse models of diabetes. J. Clin. Invest. **118**, 3378–3389
18 Preston, A. M., Gurisik, E., Bartley, C., Laybutt, D. R. and Biden, T. J. (2009) Reduced endoplasmic reticulum (ER)-to-Golgi protein trafficking contributes to ER stress in lipotoxic mouse β-cells by promoting protein overload. Diabetologia **52**, 2369–2373
19 El-Assaad, W., Buteau, J., Peyot, M. L., Nolan, C., Roduit, R., Hardy, S., Joly, E., Dbaibo, G., Rosenberg, L. and Prentki, M. (2003) Saturated fatty acids synergize with elevated glucose to cause pancreatic β-cell death. Endocrinology **144**, 4154–4163
20 Borradaile, N. M., Han, X., Harp, J. D., Gale, S. E., Ory, D. S. and Schaffer, J. E. (2006) Disruption of endoplasmic reticulum structure and integrity in lipotoxic cell death. J. Lipid Res. **47**, 2726–2737
21 Pineau, L., Colas, J., Dupont, S., Beney, L., Fleurat-Lessard, P., Berjeaud, J. M., Berges, T. and Ferreira, T. (2009) Lipid-induced ER stress: synergistic effects of sterols and saturated fatty acids. Traffic **10**, 673–690
22 Ariyama, H., Kono, N., Matsuda, S., Inoue, T. and Arai, H. (2010) Decrease in membrane phospholipid unsaturation induces unfolded protein response. J. Biol. Chem. **285**, 22027–22035
23 Paumen, M. B., Ishida, Y., Muramatsu, M., Yamamoto, M. and Honjo, T. (1997) Inhibition of carnitine palmitoyltransferase I augments sphingolipid synthesis and palmitate-induced apoptosis. J. Biol. Chem. **272**, 3324–3329
24 Pettus, B. J., Chalfant, C. E. and Hannun, Y. A. (2002) Ceramide in apoptosis: an overview and current perspectives. Biochim. Biophys. Acta **1585**, 114–125
25 Swanton, C., Marani, M., Pardo, O., Warne, P. H., Kelly, G., Sahai, E., Elustondo, F., Chang, J., Temple, J., Ahmed, A. A. et al. (2007) Regulators of mitotic arrest and ceramide metabolism are determinants of sensitivity to paclitaxel and other chemotherapeutic drugs. Cancer Cell **11**, 498–512
26 Wei, Y., Wang, D., Topczewski, F. and Pagliassotti, M. J. (2006) Saturated fatty acids induce endoplasmic reticulum stress and apoptosis independently of ceramide in liver cells. Am. J. Physiol. Endocrinol. Metab. **291**, E275–E281
27 Shimabukuro, M., Higa, M., Zhou, Y. T., Wang, M. Y., Newgard, C. B. and Unger, R. H. (1998) Lipoapoptosis in β-cells of obese prediabetic *fa*/*fa* rats. Role of serine palmitoyltransferase overexpression. J. Biol. Chem. **273**, 32487–32490
28 Shimabukuro, M., Zhou, Y. T., Levi, M. and Unger, R. H. (1998) Fatty acid-induced β-cell apoptosis: a link between obesity and diabetes. Proc. Natl. Acad. Sci. U.S.A. **95**, 2498–2502
29 Lupi, R., Dotta, F., Marselli, L., Del Guerra, S., Masini, M., Santangelo, C., Patane, G., Boggi, U., Piro, S., Anello, M. et al. (2002) Prolonged exposure to free fatty acids has cytostatic and pro-apoptotic effects on human pancreatic islets: evidence that β-cell death is caspase mediated, partially dependent on ceramide pathway, and Bcl-2 regulated. Diabetes **51**, 1437–1442
30 Beeharry, N., Chambers, J. A. and Green, I. C. (2004) Fatty acid protection from palmitic acid-induced apoptosis is lost following PI3-kinase inhibition. Apoptosis **9**, 599–607
31 Gonzalez-Pertusa, J. A., Dube, J., Valle, S. R., Rosa, T. C., Takane, K. K., Mellado-Gil, J. M., Perdomo, G., Vasavada, R. C. and Garcia-Ocana, A. (2010) Novel proapoptotic effect of hepatocyte growth factor: synergy with palmitate to cause pancreatic β-cell apoptosis. Endocrinology **151**, 1487–1498
32 Thorn, K. and Bergsten, P. (2010) Fatty acid-induced oxidation and triglyceride formation is higher in insulin-producing MIN6 cells exposed to oleate compared to palmitate. J. Cell. Biochem. **111**, 497–507

33 Bleicher, R. J. and Cabot, M. C. (2002) Glucosylceramide synthase and apoptosis. Biochim. Biophys. Acta **1585**, 172–178
34 Busch, A. K., Cordery, D., Denyer, G. S. and Biden, T. J. (2002) Expression profiling of palmitate- and oleate-regulated genes provides novel insights into the effects of chronic lipid exposure on pancreatic β-cell function. Diabetes **51**, 977–987
35 Boath, A., Graf, C., Lidome, E., Ullrich, T., Nussbaumer, P. and Bornancin, F. (2008) Regulation and traffic of ceramide 1-phosphate produced by ceramide kinase: comparative analysis to glucosylceramide and sphingomyelin. J. Biol. Chem. **283**, 8517–8526
36 Cantley, J., Burchfield, J. G., Pearson, G. L., Schmitz-Peiffer, C., Leitges, M. and Biden, T. J. (2009) Deletion of PKCε selectively enhances the amplifying pathways of glucose-stimulated insulin secretion via increased lipolysis in mouse β-cells. Diabetes **58**, 1826–1834
37 Prentki, M., Vischer, S., Glennon, M. C., Regazzi, R., Deeney, J. T. and Corkey, B. E. (1992) Malonyl-CoA and long chain acyl-CoA esters as metabolic coupling factors in nutrient-induced insulin secretion. J. Biol. Chem. **267**, 5802–5810
38 Lai, E., Bikopoulos, G., Wheeler, M. B., Rozakis-Adcock, M. and Volchuk, A. (2008) Differential activation of ER stress and apoptosis in response to chronically elevated free fatty acids in pancreatic β-cells. Am. J. Physiol. Endocrinol. Metab. **294**, E540–E550
39 Moffitt, J. H., Fielding, B. A., Evershed, R., Berstan, R., Currie, J. M. and Clark, A. (2005) Adverse physicochemical properties of tripalmitin in β-cells lead to morphological changes and lipotoxicity *in vitro*. Diabetologia **48**, 1819–1829
40 MacDonald, M. J., Dobrzyn, A., Ntambi, J. and Stoker, S. W. (2008) The role of rapid lipogenesis in insulin secretion: insulin secretagogues acutely alter lipid composition of INS-1 832/13 cells. Arch. Biochem. Biophys. **470**, 153–162
41 Lee, A. H. and Glimcher, L. H. (2009) Intersection of the unfolded protein response and hepatic lipid metabolism. Cell. Mol. Life Sci. **66**, 2835–2850
42 Sriburi, R., Jackowski, S., Mori, K. and Brewer, J. W. (2004) XBP1: a link between the unfolded protein response, lipid biosynthesis, and biogenesis of the endoplasmic reticulum. J. Cell Biol. **167**, 35–41
43 Grazide, S., Terrisse, A. D., Lerouge, S., Laurent, G. and Jaffrezou, J. P. (2004) Cytoprotective effect of glucosylceramide synthase inhibition against daunorubicin-induced apoptosis in human leukemic cell lines. J. Biol. Chem. **279**, 18256–18261
44 Li, H., Kim, W. S., Guillemin, G. J., Hill, A. F., Evin, G. and Garner, B. (2010) Modulation of amyloid precursor protein processing by synthetic ceramide analogues. Biochim. Biophys. Acta **1801**, 887–895
45 Lenzen, S. (2008) The mechanisms of alloxan- and streptozotocin-induced diabetes. Diabetologia **51**, 216–226
46 Listenberger, L. L., Han, X., Lewis, S. E., Cases, S., Farese, Jr, R. V., Ory, D. S. and Schaffer, J.E. (2003) Triglyceride accumulation protects against fatty acid-induced lipotoxicity. Proc. Natl. Acad. Sci. U.S.A. **100**, 3077–3082
47 Hodgkin, M. N., Pettitt, T. R., Martin, A., Michell, R. H., Pemberton, A. J. and Wakelam, M. J. (1998) Diacylglycerols and phosphatidates: which molecular species are intracellular messengers? Trends Biochem. Sci. **23**, 200–204
48 Lei, X., Zhang, S., Bohrer, A., Bao, S., Song, H. and Ramanadham, S. (2007) The group VIA calcium-independent phospholipase A_2 participates in ER stress-induced INS-1 insulinoma cell apoptosis by promoting ceramide generation via hydrolysis of sphingomyelins by neutral sphingomyelinase. Biochemistry **46**, 10170–10185
49 Kelpe, C. L., Moore, P. C., Parazzoli, S. D., Wicksteed, B., Rhodes, C. J. and Poitout, V. (2003) Palmitate inhibition of insulin gene expression is mediated at the transcriptional level via ceramide synthesis. J. Biol. Chem. **278**, 30015–30021
50 Medina-Gomez, G., Yetukuri, L., Velagapudi, V., Campbell, M., Blount, M., Jimenez-Linan, M., Ros, M., Oresic, M. and Vidal-Puig, A. (2009) Adaptation and failure of pancreatic β-cells in murine models with different degrees of metabolic syndrome. Dis. Model Mech. **2**, 582–592
51 Medina-Gomez, G., Gray, S. L., Yetukuri, L., Shimomura, K., Virtue, S., Campbell, M., Curtis, R. K., Jimenez-Linan, M., Blount, M., Yeo, G. S. et al. (2007) PPARγ2 prevents lipotoxicity by controlling adipose tissue expandability and peripheral lipid metabolism. PLoS Genet. **3**, e64
52 Sauane, M., Su, Z. Z., Dash, R., Liu, X., Norris, J. S., Sarkar, D., Lee, S. G., Allegood, J. C., Dent, P., Spiegel, S. and Fisher, P. B. (2010) Ceramide plays a prominent role in MDA-7/IL-24-induced cancer-specific apoptosis. J. Cell. Physiol. **222**, 546–555
53 Moore, P. C., Ugas, M. A., Hagman, D. K., Parazzoli, S. D. and Poitout, V. (2004) Evidence against the involvement of oxidative stress in fatty acid inhibition of insulin secretion. Diabetes **53**, 2610–2616
54 Carlsson, C., Borg, L. A. and Welsh, N. (1999) Sodium palmitate induces partial mitochondrial uncoupling and reactive oxygen species in rat pancreatic islets *in vitro*. Endocrinology **140**, 3422–3428
55 Maestre, I., Jordan, J., Calvo, S., Reig, J. A., Cena, V., Soria, B., Prentki, M. and Roche, E. (2003) Mitochondrial dysfunction is involved in apoptosis induced by serum withdrawal and fatty acids in the β-cell line INS-1. Endocrinology **144**, 335–345
56 Wang, X., Li, H., De Leo, D., Guo, W., Koshkin, V., Fantus, I. G., Giacca, A., Chan, C. B., Der, S. and Wheeler, M. B. (2004) Gene and protein kinase expression profiling of reactive oxygen species-associated lipotoxicity in the pancreatic β-cell line MIN6. Diabetes **53**, 129–140
57 Oprescu, A. I., Bikopoulos, G., Naassan, A., Allister, E. M., Tang, C., Park, E., Uchino, H., Lewis, G. F., Fantus, I. G., Rozakis-Adcock, M. et al. (2007) Free fatty acid-induced reduction in glucose-stimulated insulin secretion: evidence for a role of oxidative stress *in vitro* and *in vivo*. Diabetes **56**, 2927–2937
58 Zhou, Y. P. and Grill, V. E. (1994) Long-term exposure of rat pancreatic islets to fatty acids inhibits glucose-induced insulin secretion and biosynthesis through a glucose fatty acid cycle. J. Clin. Invest. **93**, 870–876

Received 16 November 2010/20 January 2011; accepted 25 January 2011
Published as BJ Immediate Publication 25 January 2011, doi:10.1042/BJ20101867

Biochem. J. (2011) **435**, 267–276 (Printed in Great Britain) doi:10.1042/BJ20101867

online data

SUPPLEMENTARY ONLINE DATA

A lipidomic screen of palmitate-treated MIN6 β-cells links sphingolipid metabolites with endoplasmic reticulum (ER) stress and impaired protein trafficking

Ebru BOSLEM*†, Gemma MacINTOSH‡, Amanda M. PRESTON*†, Clarissa BARTLEY*, Anna K. BUSCH*, Maria FULLER§, D. Ross LAYBUTT*†, Peter J. MEIKLE‡ and Trevor J. BIDEN*†[1]

*Diabetes and Obesity Program, Garvan Institute of Medical Research, 384 Victoria Street, Darlinghurst, NSW 2010, Australia, †St Vincent's Clinical School, Faculty of Medicine, University of New South Wales, Sydney, NSW, Australia, ‡Baker IDI Heart and Diabetes Institute, Commercial Road, Melbourne, Australia, and §Department of Genetic Medicine, Children, Youth and Women's Health Service, 72 King William Road, Adelaide, SA 5006, Australia

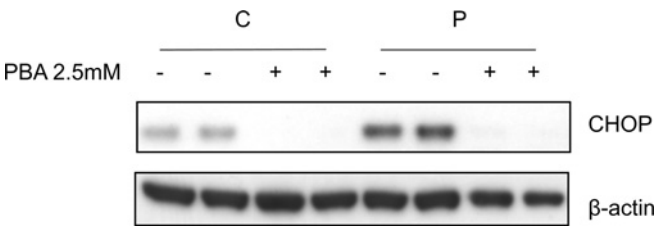

Figure S1 PBA inhibits ER stress in response to palmitate

A representative blot showing the inhibition of the ER stress transducer CHOP in the presence (+) or absence (−) of PBA (2.5 mM) during chronic palmitate treatment (0.4 mM palmitate and 0.92 g/100 ml BSA). Control groups were treated with BSA alone.

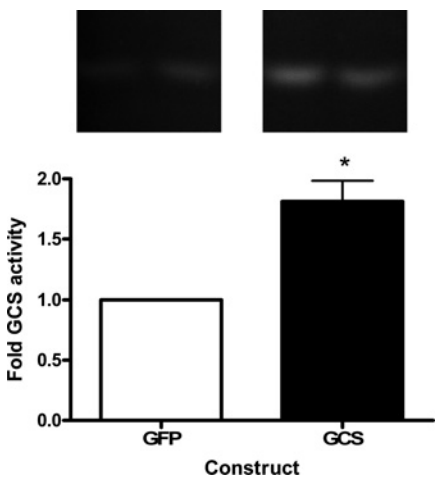

Figure S2 Overexpression of GCS increases metabolic flux of ceramide into GlcCer

A representative image of the TLC plate and densitometric analysis (ImageJ software) of the intensity of fluorescent NBD–Cer conversion into NBD–GlcCer from MIN6 cell extracts transfected with GCS or GFP control constructs. Values are mean fold GCS activity (calibrated absorbance of signal) +S.E.M. for three independent experiments. $^*P < 0.05$, using Student's paired *t* test).

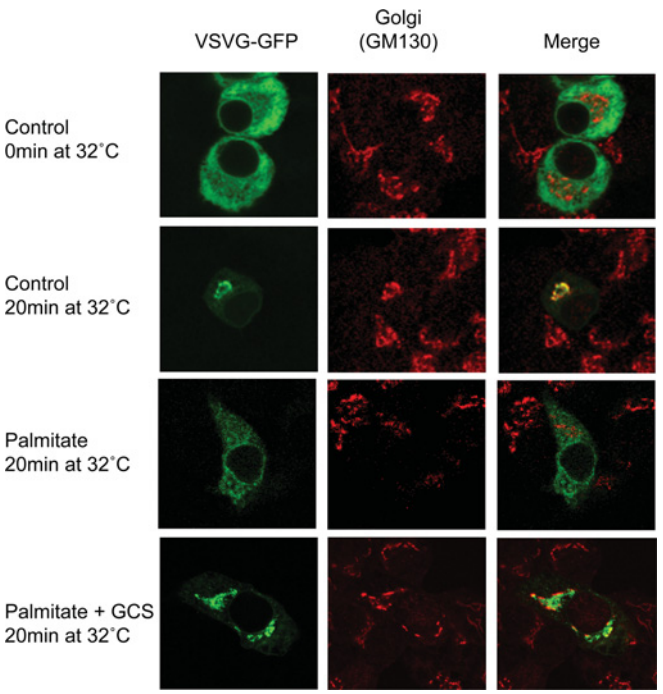

Figure S3 Overexpression of GCS protects MIN6 cells against defective protein trafficking due to chronic palmitate treatment

Cells were transfected with VSVG (as well as GCS where indicated) and then treated for 48 h with 0.4 mM palmitate and 0.92 g/100 ml BSA or BSA alone. Prior to the experiment, cells were incubated overnight at 40 °C to trap VSVG in the ER. Following brief pre-treatment with cycloheximide to halt new protein synthesis, the cells were switched to 32 °C to allow trafficking of VSVG to the ER over 20 min. Representative panels of subcellular localization of VSVG and Golgi marker GM130 in MIN6 cells are shown for the times and conditions indicated.

Received 16 November 2010/20 January 2011; accepted 25 January 2011
Published as BJ Immediate Publication 25 January 2011, doi:10.1042/BJ20101867

[1] To whom correspondence should be addressed (email t.biden@garvan.org.au).